Rev.Adv.Mater.Sci. 18(2008) 190-192

DEVELOPING Au-BASED AMORPHOUS ALLOYS

Gianluca Fiore and Livio Battezzati

Dipartimento di Chimica IFM e Centro di Eccellenza NIS, Universita di Torino, Via P. Giuria 7, 10125 Torino, Italy

Received: March 29, 2008

Abstract. The present work is aimed at exploring new systems, close to 18 karat gold, for the synthesis of amorphous alloys. Results are reported on glass-forming tendency, microstructure and stability of various compositions in the Au-Cu-Si, Au-Cu-Ti-Si and Au-Cu-Y systems. Glass formation has been achieved in Au-Cu-Si at a composition corresponding to the minimum of the mixing enthalpy in the liquid state, whereas formation of unknown intermetallics limit the quenchability of Au-Cu-Y.

1. INTRODUCTION

Metallic glasses have attracted interest because of their high strengh, good resistence to corrosion, high elastic energy, high hardness and net shape surface. Roughness of amorphous alloys can be decreased up to the nanometer scale. This property is very important in the jewellery field. Therefore, it can be possible to decrease manufacturing cost, e.g. polishing, using amorphous materials.

After the pioneering work on Au-Si which paved the way to amorphisation by rapid quenching molten alloys [1], the topic of Au-based glassy alloys has seen a resurgence of interest only in recent times with the discovery of a bulk metallic glass of new composition [2]. The aim of this works is to explore new compositions.

In 1997 it was shown that the composition $Au_{37.5}Cu_{37.5}Si_{25}$ corresponds to the minimun negative excess Gibbs free energies of formation at 1750K, suggesting better glass forming tendency [3]. This alloy was melt spun for to check amorphization in order to obtain a composition close to 18 carat; then part of Si was replaced with Ti, because Ti has a strong negative heat mixing with Au: the result is $Au_{42}Cu_{29}Si_{21}Ti_{8}$.

In the same way, after reproducing the result of Giessen *et al.* [4] for $Au_{80}Cu_{10}Y_{10}$, we changed the composition to $Au_{52}Cu_{36}Y_{12}$ corresponding to 18 carat gold alloy.

Finally, noting that the alloy $Cu_{60}Ti_{30}Zr_{10}$ is a good glass-former [5], some of Cu was replaced with Au [6] to check for the glass-forming tendency [7].

2. EXPERIMENTAL

Samples were prepared by arc-melting the pure elements (Au: 99.999%, Cu: 99.99%, Si: 99.9995%, Y: 99.9%, Ti:99.9%, Zr:99.8%) in an argon atmosfere. Portions of master alloys were rapidly quenched in a melt spinning apparatus under Ar to produce ribbons some tens of micron thick.

Phase trasformations were studied by differential scanning calorimetry (DSC) at the heating rate of 0.33 K/s. All DSC runs were perfomed under flowing Ar. The structure of the samples was examined by X-ray diffraction (XRD) with monochromatic Cu K_{α} radiation. Microstructures of the samples were investigated with optical microscopy and scanning electron microscopy (SEM).

3. RESULT AND DISCUSSION

3.1. $Au_{37.5}Cu_{37.5}Si_{25}$ (ACS)

As shown in the XRD pattern of Fig. 1, the structure of the as-solidified ACS alloy is partially amor-

Corresponding author: Gianluca Fiore, e-mail: gianluca.fiore@unito.it

Table 1. Summary of the thermal properties of the alloys.

Sample	$T_{g\ onset}$ [K]	$T_{g\ end}$ [K]	T_x [K]	ΔH_x [J/g]	T_m [K]	T_l [K]
ACS	-	-	412	24	635	~ 1073
ACST	393	404	413	9.3	763	1168
ACTZ	-	-	754	55	1184	1738

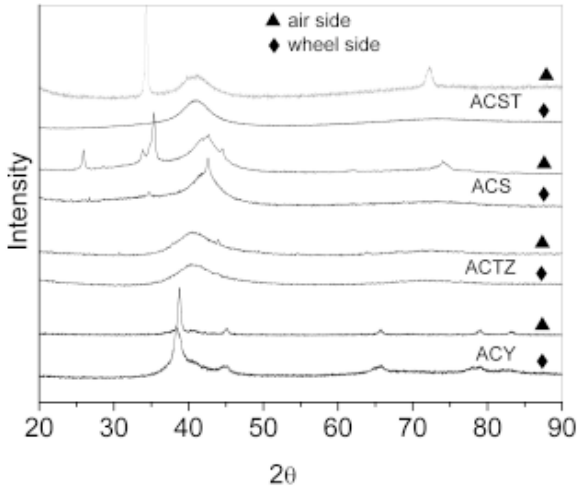

Fig. 1. XRD patterns of the alloys in ribbon form.

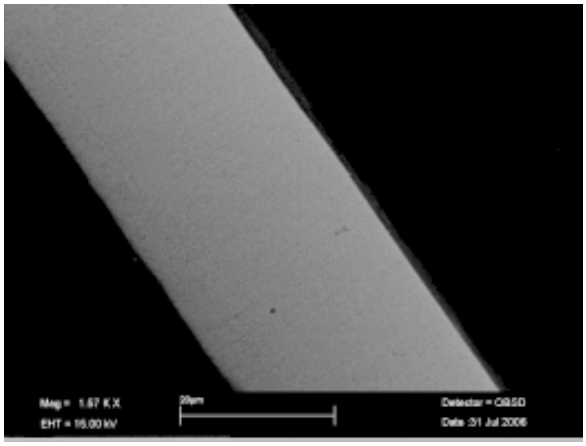

Fig. 2. SEM micrograph (backscattered electrons) of ACS ribbon in cross section.

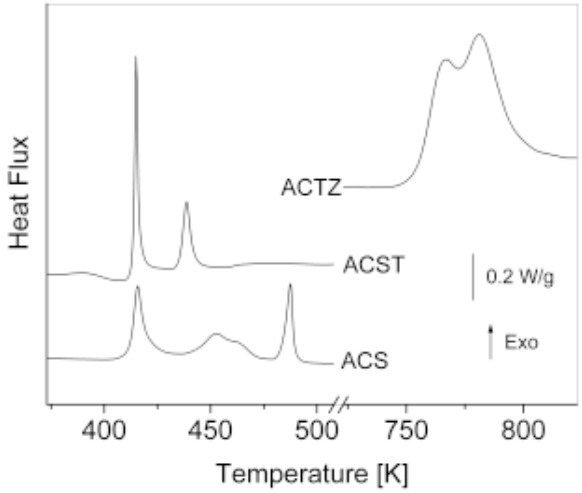

Fig. 3. DSC traces of the ribbons ACS, ACST and ACTZ, determinated at 0.33 K/s.

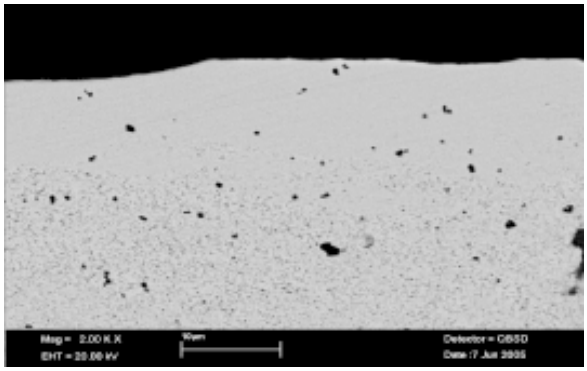

Fig. 4. SEM micrograph (backscattered electrons) of ACST ribbon in cross section.

Fig. 5. Optical micrograph of ACY1 (ribbon etche with aqua regia).

phous. The peaks are associated with some unknow crystalline phase. Backscattered electron microscopy analysis of the ribbon cross section (Fig. 2) does not show phase contrast, therefore the size of crystallites can be of nanometer order. The DSC trace of the sample (Fig. 3) has three exothermic peaks showing the devitrification of the amorphous phase similar by to previous Au-Cu-Ge-Si alloys [8]. No clear evidence of the glass tran-

sition T_g has been identified, because of the prevalence of crystallization at around 403K (Table 1).

3.2. $Au_{42}Cu_{29}Si_{21}Ti_8$ (ACST)

On the wheel side the diffraction pattern consists of a glassy phase (Fig. 1), whereas on the air side there are sharp signals in addition to the halo of the amorphous matrix. This is also shown in Fig. 4: the ribbon can be divided in two different zones: the wheel zone where there are few precipitates, and the air zone where the amount of precipitates is larger.

DSC experiments (Fig. 3) confirm the amorphous state of the sample since T_g is apparent at 393K. In Table 1 thermal properties are summarized: $T_{g\ \mathrm{onset}}$ (start of the glass transition temperature), $T_{g\ \mathrm{end}}$ (end of the glass transition temperature), T_x (crystallization temperature), ΔH_x (heat of crystallization), T_m (melting temperature) and T_l (liquidus temperature).

3.3. $Au_{80}Cu_{10}Y_{10}$ (ACY1) – $Au_{52}Cu_{36}Y_{12}$ (ACY2)

The ribbon structure of the alloy ACY1 is mostly crystalline as confirmed by XRD pattern (Fig. 1). Optical microscopy of the etched ribbon (Fig. 5) shows a fine microstructure and a featureless part on the wheel side; this can be the cause of the low intensity halo in the diffraction pattern. The sample is subject to strong oxidation on heating, so the calorimetric signal (not reported) is a monotonically increasing line. Changing the composition to ACY2, the ribbon becomes fully crystalline with formation of unknown ternary intermetallics that strongly limit the quenchability of the alloy.

3.4 $Au_{22}Cu_{38}Ti_{30}Zr_{10}$ (ACTZ)

XRD patterns (Fig. 1) of the as-spun ribbon show fully amorphous state for the wheel side and partially for the other side.

Analyzing the ribbon cross section with backscattered electrons no evidence of microstructure were observed, confirming the amorphicity of the sample.

Two distinct exotermic peaks were observed in the DSC curve, associated with crystallization of the glassy phase. The glass transition was not evidenced. The trasformation temperature are much higher than in previous cases, following the trend of the liquidus temperature (Table 1).

4. CONCLUSION

Four alloys have been processed by melt spinning and their structure has been studied with XRD, DSC and SEM.

The $Au_{37.5}Cu_{37.5}Si_{25}$ alloys is partially amorphous. $Au_{42}Cu_{29}Si_{21}Ti_8$ is amorphous on wheel side whereas on the air side contains several precipitates. The amorphization of the third alloy ($Au_{80}Cu_{10}Y_{10}$) is limited by formation of intermetallic compounds. The tendence to amorphization of $Au_{22}Cu_{38}Ti_{30}Zr_{10}$ is very good, however the alloy is constituted by high melting intermetallics.

ACKNOWLEDGEMENTS

Research on metallic glasses is performed within the “Bando Regionale Ricerca Scientifica Applicata 2004, progetto D23”.

REFERENCES

[1] W. Klement jr., R. H. Willens and P. Duwez // *Nature* **187** (1960) 869.
[2] J. Schoers, B. Lohwongwatana, W. L. Johnson and A. Peker // *Appl. Phys. Lett.* **87** (2005) 061912.
[3] C. Bergman, R. Chastel and J. C. Mathieu // *Thermochim. Acta* **314** (1998) 169.
[4] B.C. Giessen, S.V. Gokhale and K.G. Marchev, *Patent number 5,593,514.*
[5] E.S. Park, H.J. Chang, D.H. Kim, W.T. Kim, Y.C. Kim and N.J. Kim // *Scripta Materialia* **51** (2004) 221.
[6] D.V. Louzguine and A. Inoue // *Journal of Alloys and Compounds* **361** (2003) 153.
[7] L. Battezzati, G.L. Fiore and M. Massazza // *J. Metast. Nanocryst. Material* **24-25** (2005) 37.
[8] C.V. Thompson, A.L. Greer and F. Spaepen // *Acta Metall* **31** (1983) 1883.